The IMAT camera and energy-selective imaging

National Research Council of Italy

G.Salvato

CNR-IPCF Messina

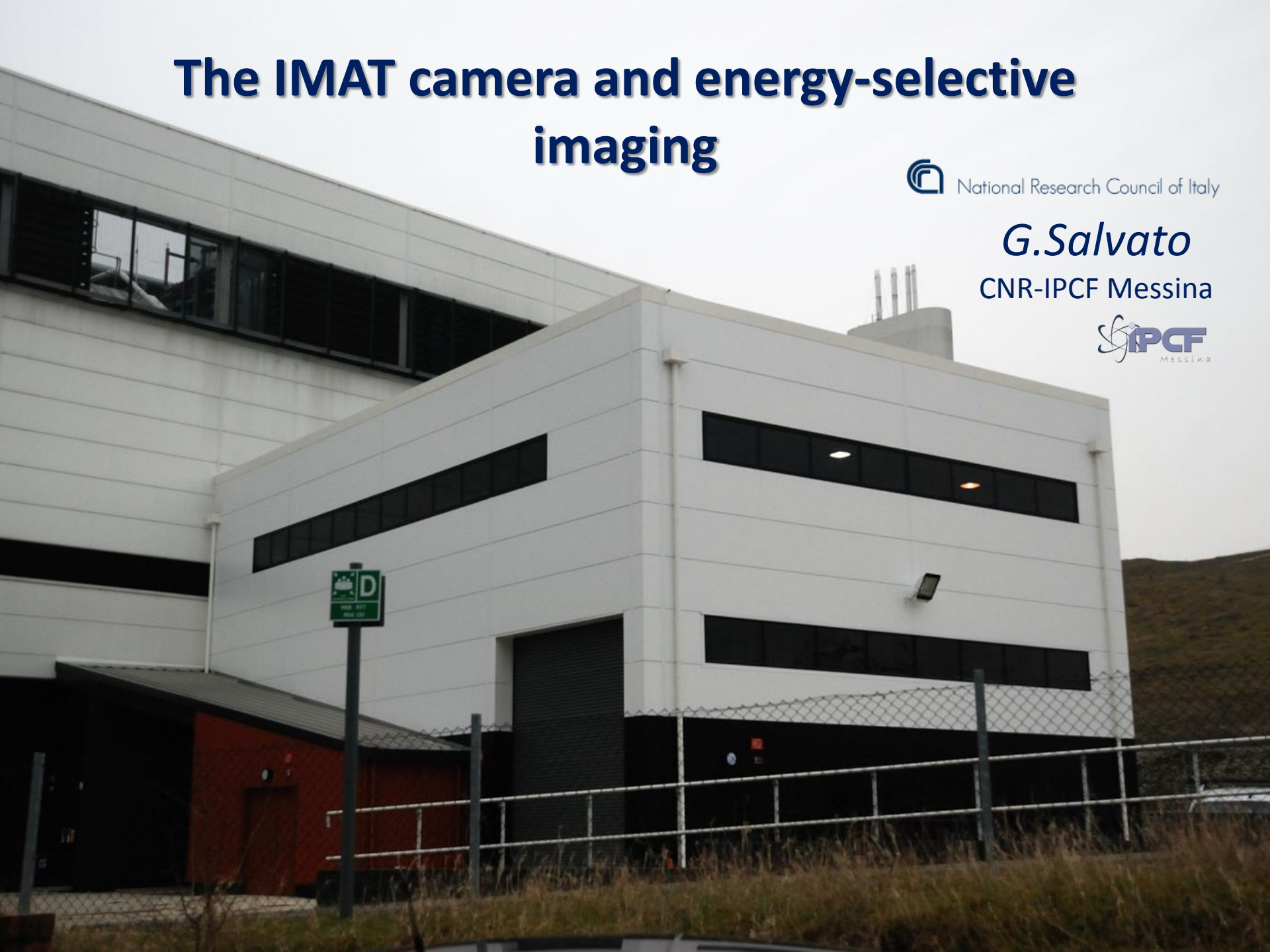

National Research Council of Italy

IPCF Messina

Science & Technology Facilities Council

At IMAT two different operative modes will be available:

Neutron Imaging

Conventional (white-beam) **Radiography/ Tomography**

Energy Selective Imaging

Diffraction

Phase analysis

Strain & Stress

Texture

The IMAT beamline

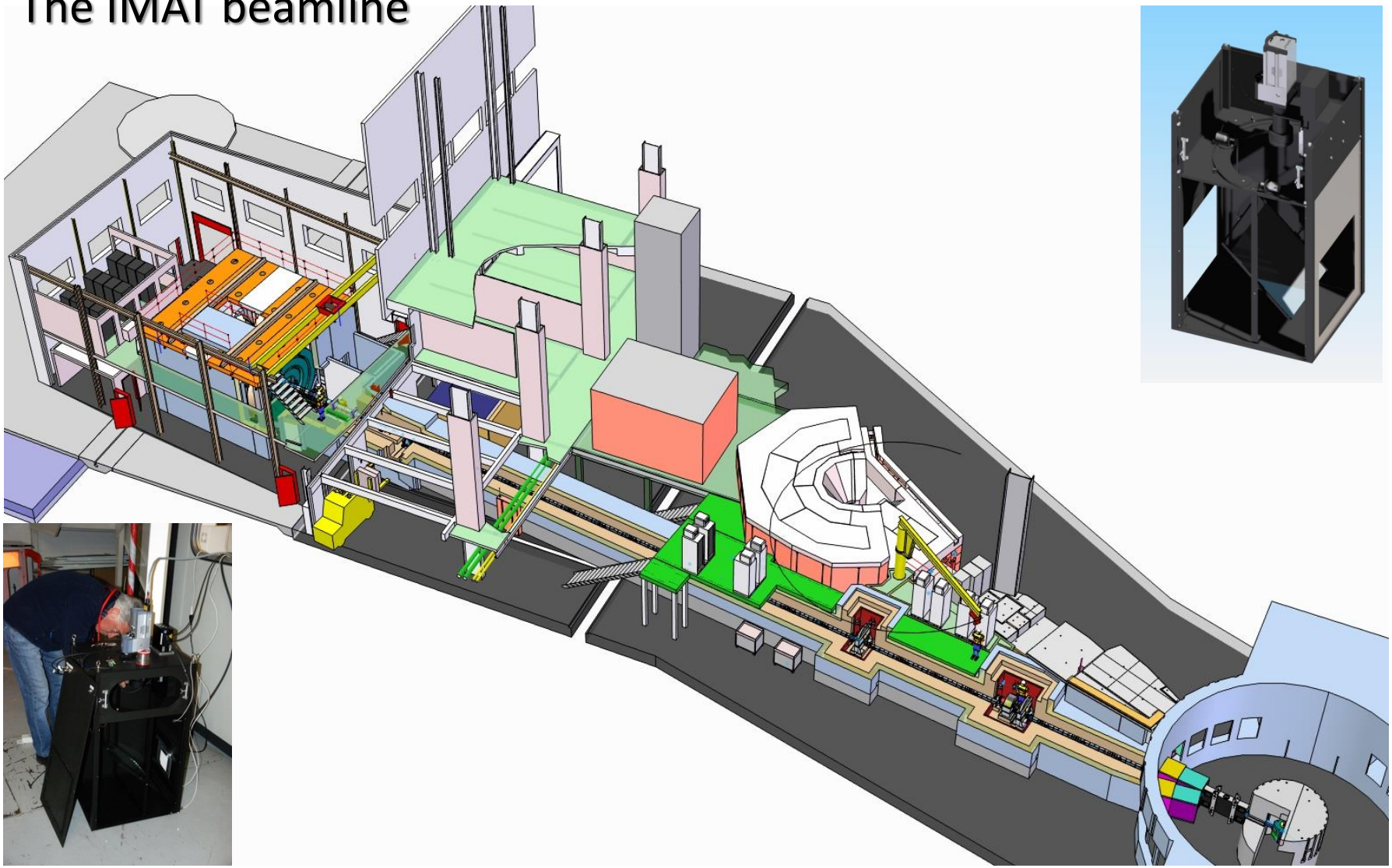

Repetition rate	10 Hz
Flight path	56m to sample
Single frame bandwidth	0.7 - 7 Å
Double frame bandwidth	2 - 14 Å
Neutron flux	~ 10^7 n/cm^2/sec
L/D	2000, 1000, 500, 250, 125
Maximum Field of View	20x20 cm
Spatial resolution	50 – 200 µm
Wavelength resolution	$\Delta\lambda/\lambda$= 0.7 % (at 3 Å)

First neutron in 2015 !

The transmission of a neutron beam through a sample is described by the *Lambert-Beer* law:

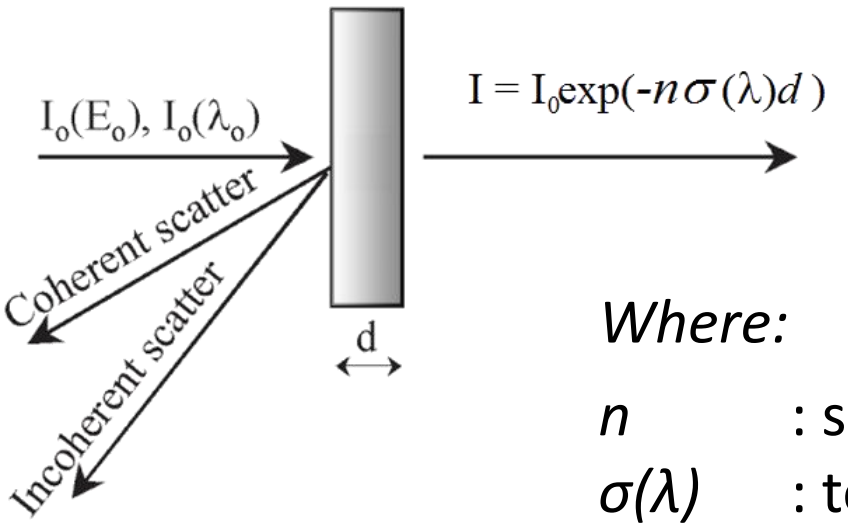

$$I(\lambda) = I_0(\lambda)e^{-n\sigma(\lambda)d}$$

Where:

n : scattering center number.

σ(λ) : total cross-section per scattering center.

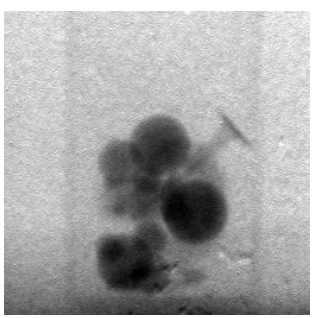

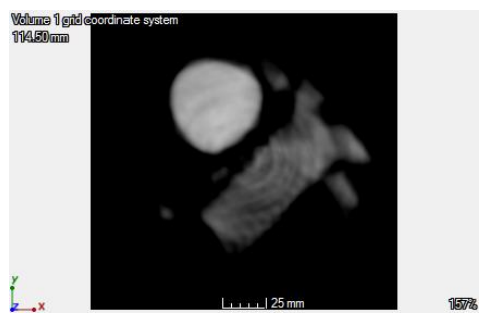

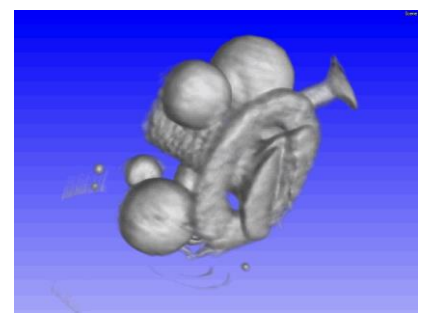

At a pulsed neutron source (e.g. ISIS - UK) the neutrons are produced in bunches at precise time intervals.

The arrival time of the neutron at the detector (measured from each of the production instants) depends on its energy or, equivalently, on its wavelength.

This "**Time of Flight**" (TOF), from moderator to detector, is tied to the neutron wavelength by:

$$t = (m\,L / h)\ \lambda$$

where:

m = neutron mass
h = Planck constant
L = flight path

Please keep in mind that
TOF is directly proportional to the wavelength.

To get an idea of the numbers involved:

neutrons with a

wavelength, $\boldsymbol{\lambda = 1\text{Å} = 10^{-10}\ \mathrm{m}}$

and a

flight path, $\boldsymbol{L = 30\ \mathrm{m}}$

have a

TOF $\boldsymbol{t \approx 7.585\ \mathrm{ms}}$

At pulsed sources, it is very easy to determine the wavelength of a neutron by examining its traveling time.

To determine the structure of a polycrystalline sample by ***neutron diffraction***, a wavelength-dependent intensity spectrum is recorded under some angle to the direction of the incident neutron beam.

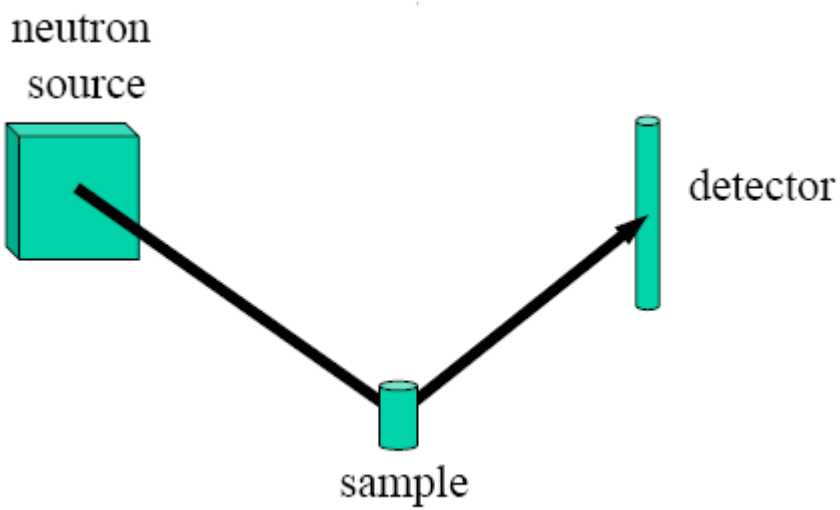

At certain TOFs (wavelengths) strong intensity maxima are detected: the ***Bragg peaks***.

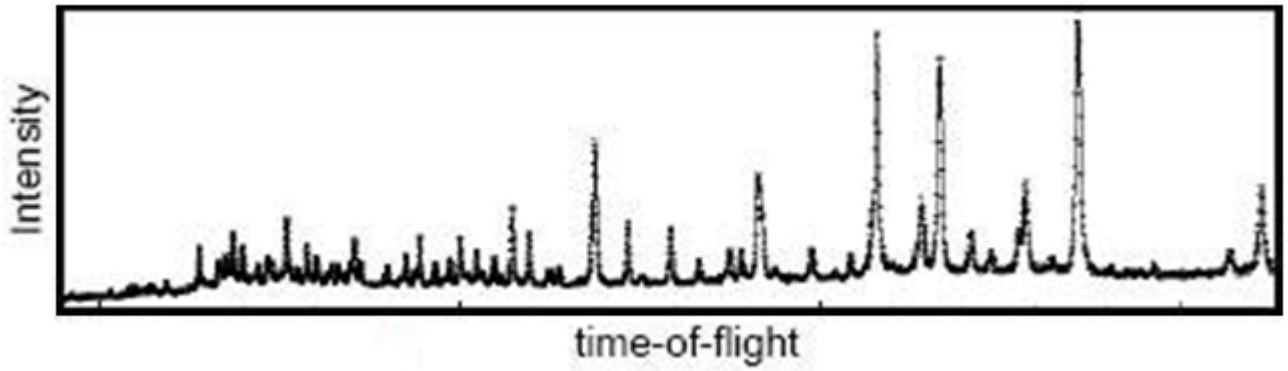

R.Smith
"Powder Diffraction"

Bragg's Law

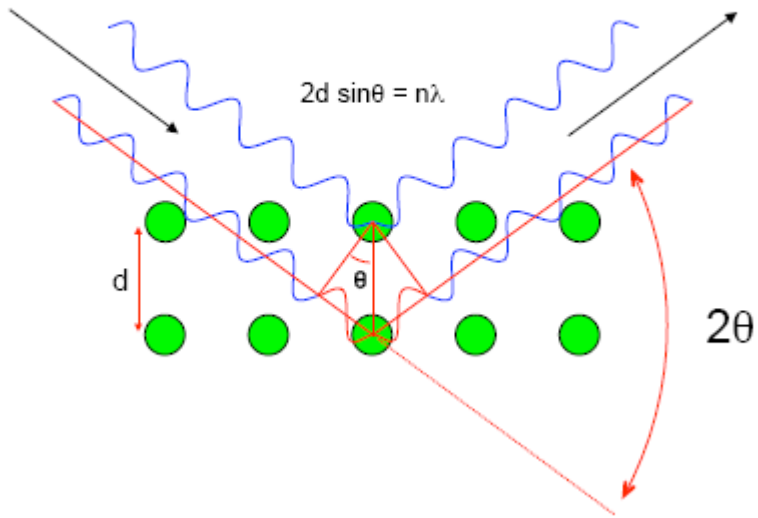

$$n \cdot \lambda = 2 \cdot d \cdot \sin\theta$$

$\boldsymbol{d}$	is the interplanar distance
$\boldsymbol{2\theta}$	is the scattering angle
$\boldsymbol{n}$	$= 1, 2, \ldots$

Example: ***Cu - fcc,***

<u>lattice Constant</u>: ***a*=3.610** Å

<u>detector</u> @ 2θ = **90°**

$$d_{hkl} = \frac{a}{\sqrt{h^2 + k^2 + l^2}}$$

$$d_{220} = \frac{3.610}{\sqrt{2^2 + 2^2 + 0^2}} = 1.276\,[\text{Å}]$$

$$n \cdot \lambda = 2 \cdot d \cdot \sin\theta$$

$$n \cdot \lambda = 2 \cdot d_{220} \cdot \sin 45° \cong 2 \cdot 1.276 \cdot 0.707 = 1.8045\,[\text{Å}]$$

we will have peaks at ***λ*=1.8045**, **0.9023**, … **[Å]**.

if the ***flight path***= **30 m** the corresponding ***TOFs*** are**:**

13.686, **6.8435,** … **ms**

A large fraction of neutrons remains unused since, usually, only a small solid angle is covered with detectors but the neutrons are scattered over 4π.

The scattered neutrons are removed from the direct beam path and, placing a detector just beyond the sample, **will not contribute to the measured signal**.

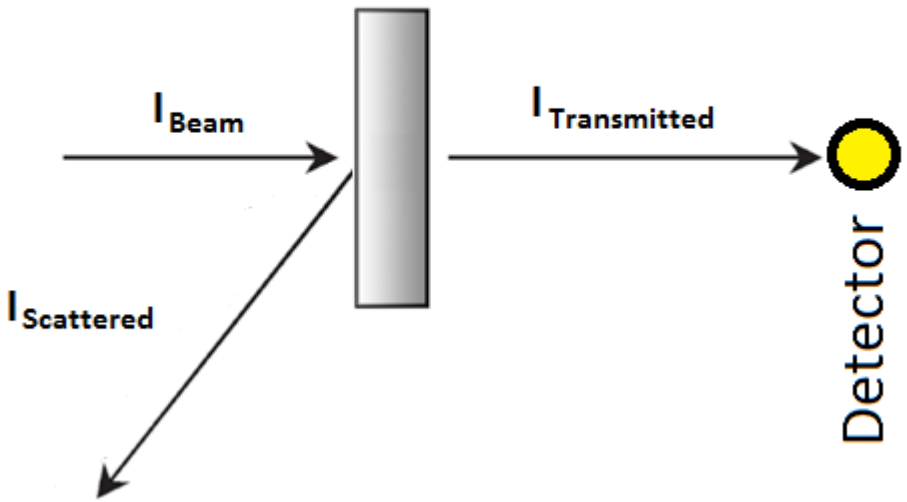

$$I_{Transmitted} \leq I_{Beam}$$

For a given *hkl* reflection, the *Bragg* angle increases as the wavelength increases **until 2θ is equal to 180°**.

At wavelengths greater than this critical value, no scattering by this particular *{hkl}* family can occur and there is thus an increase in the transmitted intensity.

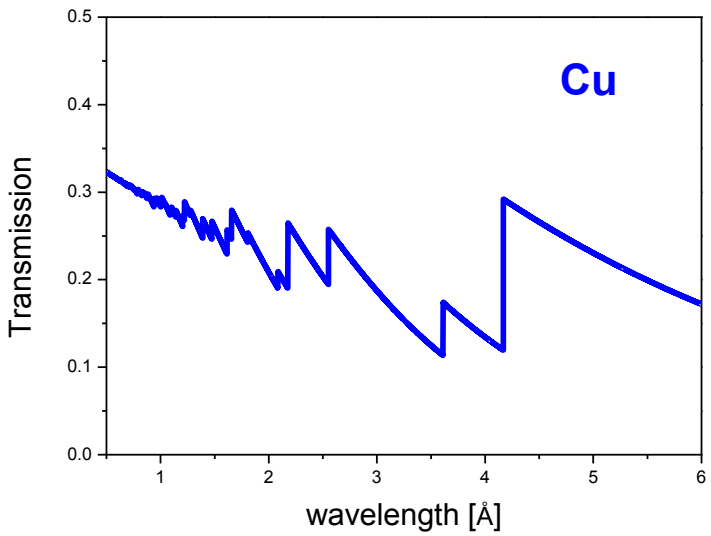

From *Bragg's* law, the wavelength at which this occurs is:

$$\lambda = 2d_{hkl}$$

giving a measure of the *{hkl}* *d*-spacing in the direction of the incoming beam.

Please keep in mind that
the wavelength is directly proportional to the TOF.

To investigate production processes and/or induced or residual strains we should be able to detect small variations in *d*-spacing.

Required accuracies are in the order of $\frac{\Delta d}{d} \cong 0.01\%$

The detectable strain, ε, is tied to the accurate determination of the time at which the Bragg edge occurs.

$$\varepsilon_{hkl} = \frac{d_{hkl} - {d^0}_{hkl}}{{d^0}_{hkl}} = \frac{t_{hkl} - {t^0}_{hkl}}{{t^0}_{hkl}} = \frac{\Delta t_{hkl}}{{t^0}_{hkl}} \sim 10^{-4}$$

Where ${d^0}_{hkl}$ and ${t^0}_{hkl}$ are the *unstrained* quantities

If ${t^0}_{hkl} \sim 10ms$ then ***we should discriminate Δt~10μs***

We need a good model of the Bragg-edge profile!

$$\frac{I(\lambda)}{I_0(\lambda)} = e^{-n\sigma(\lambda)d}$$

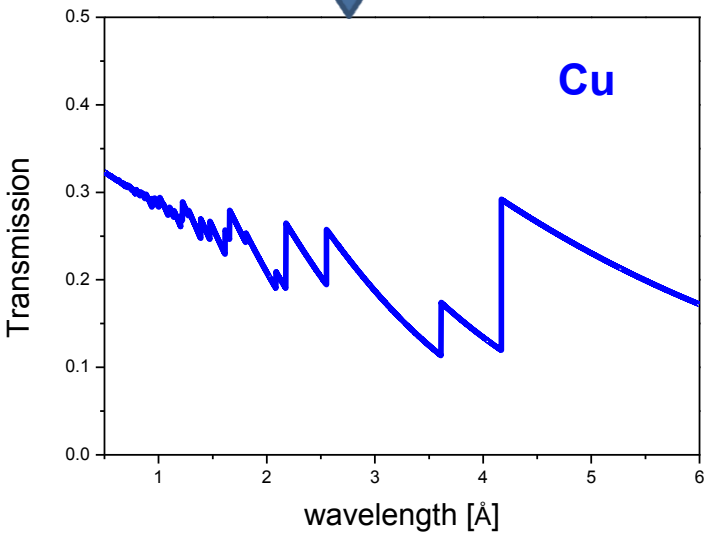

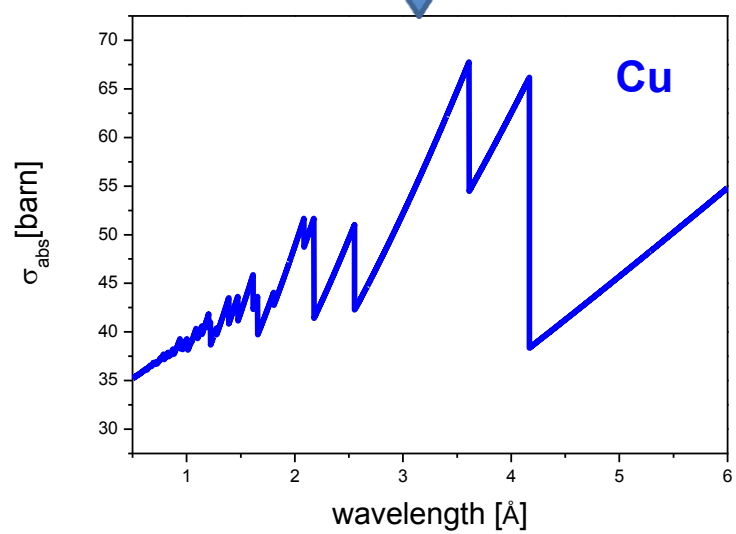

We can express mathematically the total cross section as:

$$\sigma_{tot}(\lambda) = \sigma(\lambda) + \sum_{hkl} \sigma_{hkl(\lambda)}[1 - u(\lambda - 2d_{hkl})]$$

Where *u(.)* is the Heaviside step function.

In a real experiment, the measured edge profiles differ from the ideal ones.

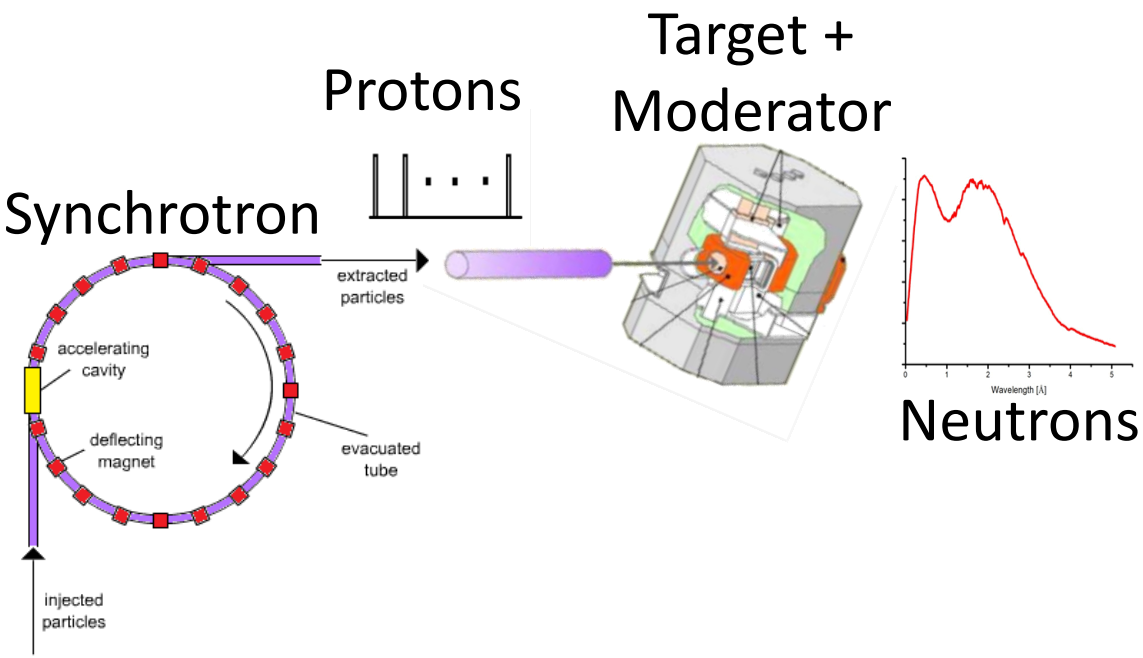

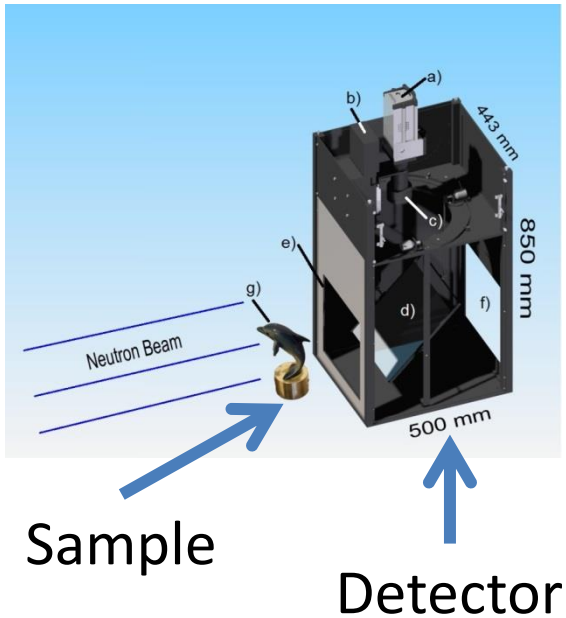

The proton pulses are very short ~ 100ns and produce high energy neutrons. The neutron energy must be reduced to be useful for materials investigation.

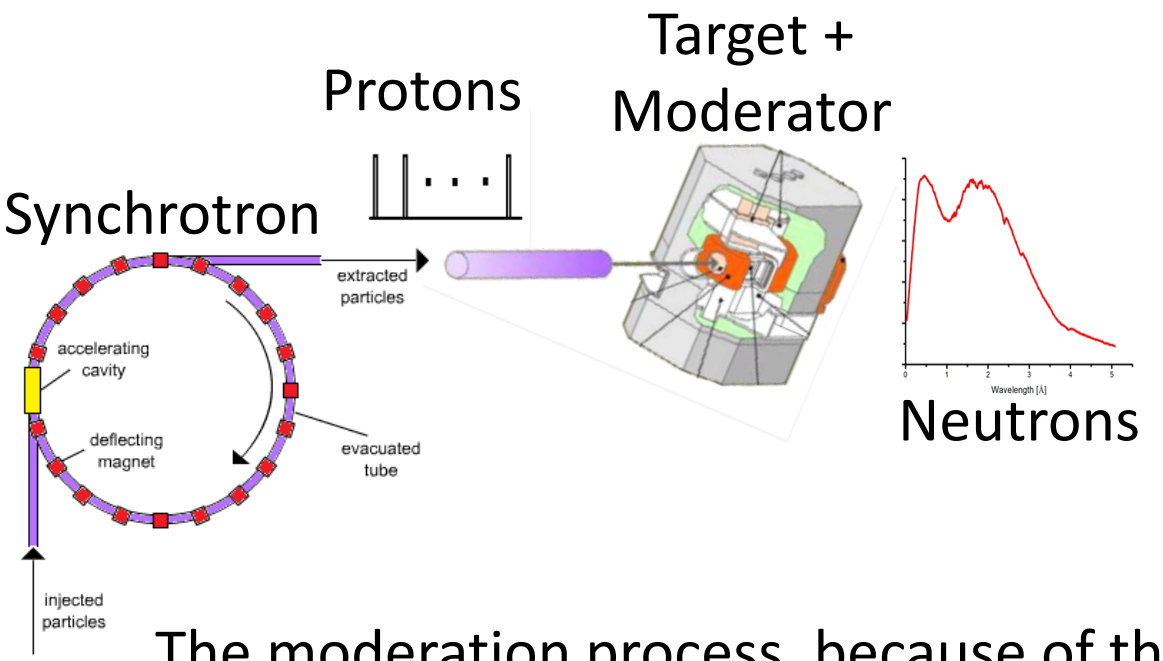

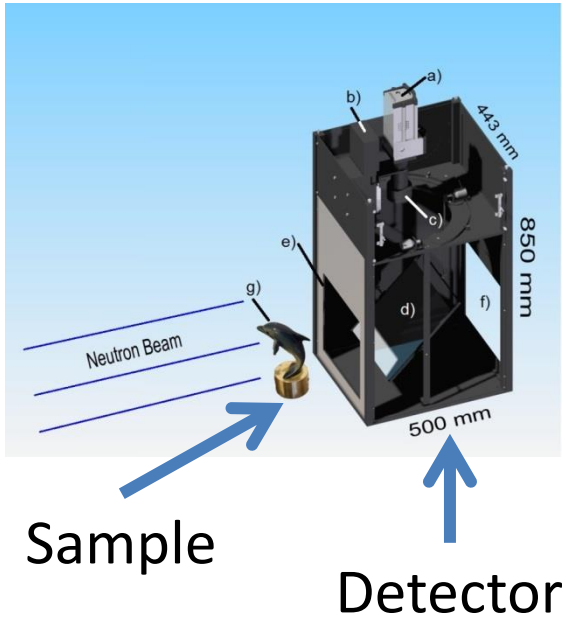

The moderation process, because of the collisions with the moderator atoms, reduces the neutron energy but introduces an ***uncertainty*** on the time and position at which the neutron leaves the moderator. We can express such a circumstance with a (<u>sharply peaked</u>)

instrument resolution function *R(λ,t).*

With the assumption: $\int_0^\infty R(\lambda', t) d\lambda' = 1$

Neutrons leaving the moderator have a <u>very broad wavelength distribution</u>: $\boldsymbol{S(\lambda)}$

We can express mathematically the number of neutrons, $\boldsymbol{N_{in}(t)}$, detected between $\boldsymbol{t}$ and $\boldsymbol{t+\Delta t}$ <u>when the sample is in the beam</u>:

$$\boxed{N_{in}(t) = I_{in}(t)\Delta t = \left[\int_0^{\infty} S(\lambda')\, R(\lambda', t)\varepsilon(\lambda')Tr(\lambda')d\lambda'\right]\Delta t}$$

$\boldsymbol{\varepsilon(\lambda)}$ is the detector efficiency

$\boldsymbol{Tr(\lambda)} = e^{-nw\sigma_{tot}(\lambda)}$ is the transmission of the sample

n is the number of atoms per unit volume

w is the sample thickness

$\sigma_{tot}(\lambda)$ is the total cross section

Remembering the expression for the cross section,

$$\sigma_{tot}(\lambda) = \sigma(\lambda) + \sum_{hkl} \sigma_{hkl(\lambda)}[1 - u(\lambda - 2d_{hkl})]$$

we can isolate a single edge tied to the *hkl* plane family:

$$\sigma_{tot}(\lambda) = \sigma_0(\lambda) + \sigma_{hkl}(\lambda)[1 - u(\lambda - 2d_{hkl})]$$

where $\sigma_0(\lambda)$ accounts for contributions other than the elastic coherent scattering of the current *hkl*.

In the narrow wavelength range in which $R(\lambda,t)$ differs from zero, the slow varying $S(\lambda)$, $\varepsilon(\lambda)$ and $\sigma_0(\lambda)$ can be taken outside the integral:

Remembering the:

$$N_{in}(t) = I_{in}(t)\Delta t = \left[\int_0^\infty S(\lambda')\, R(\lambda', t)\varepsilon(\lambda')Tr(\lambda')d\lambda'\right]\Delta t$$

We can write the measured intensity: $I_{in}(t) \approx$

$$S(\lambda_t)\varepsilon(\lambda_t)e^{-nw\sigma_0(\lambda_t)}\int_0^\infty e^{-\{nw\sigma_{hkl}(\lambda')[1-u(\lambda'-2d_{hkl})]\}}R(\lambda', t)d\lambda'$$

Recalling, once more, the relationship between time of flight and wavelength

$$t = (m\ L\ /\ h)\ \lambda_t$$

The measured transmitted intensity, $I_{in}(t)$, normalized to the incident intensity, measured without the sample, $I_{out}(t)$ (=$S(\lambda_t)\varepsilon(\lambda_t)$) can be written (see [1]):

$$I_{in}(t) \Big/ I_{out}(t) \approx$$

$$e^{-nw\sigma_0(\lambda_t)}\left[e^{-nw\sigma_{hkl}(\lambda_t)} + \left(1 - e^{-nw\sigma_{hkl}(\lambda_t)}\right)\int_{2d_{hkl}}^{\infty} R(\lambda', t)d\lambda'\right]$$

by introducing explicitly the step function and assuming that also $\sigma_{hkl}(\lambda_t)$ is slowly varying with λ.

This shows that ***the measured shape of the edge depends on the instruments resolution function***.

[1] Santisteban et al. J. Appl. Cryst. **34**, 289-297 (2001)

A possible model of the resolution function, that has been found accurate enough to model the peak shapes at the ENGIN-X facility of ISIS, is due to Kropff et al. [1].

In this model, $R(\lambda, t)$ is modeled as the convolution between a Gaussian and a decaying exponential starting at $\boldsymbol{t_0(\lambda)}$ with a time constant $\boldsymbol{\tau(\lambda)}$:

$$R(\lambda, t) = \frac{1}{\tau(\lambda)} e^{-\frac{t-t_0}{\tau(\lambda)}} \, u(t - t_0) \quad \circledast \quad \frac{1}{\sqrt{2\pi}\sigma(\lambda)} e^{-\frac{(t-t_0)^2}{2\sigma(\lambda)^2}}$$

The advantage of this model is that it can be analytically integrated:

[1] *F. Kropff et al.* (1982). Nucl. Instrum. and Methods, **198**, 515 (1982).

$$\int_{2d_{hkl}}^{\infty} R(\lambda', t) d\lambda' =$$

$$\frac{1}{2}\left[erfc\left(-\frac{t - t_{hkl}}{\sqrt{2}\sigma}\right) - exp\left(-\frac{(t - t_{hkl})^2}{\tau} + \frac{\sigma^2}{\tau^2}\right) erfc\left(-\frac{t - t_{hkl}}{\sqrt{2}\sigma} + \frac{\sigma}{\tau}\right)\right]$$

Where $erfc(x) = 1 - erf(x) = 1 - \frac{2}{\pi}\int_0^x e^{-t^2} dt$

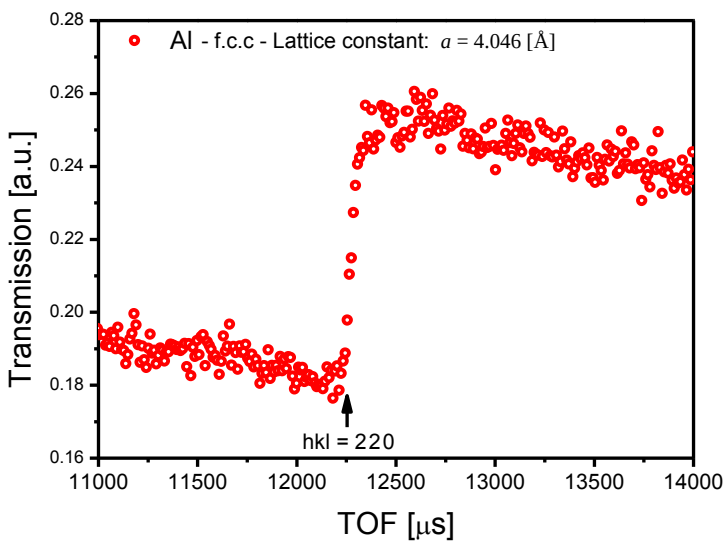

On the left we can see the *220* edge of an Al plate, as measured at ROTAX (ISIS).

It seems reasonable to approximate the cross sections σ_0 and σ_{hkl} in a small region around the edge with two linear functions:

$$nw\sigma_0 = a_0 + b_0 t \qquad nw\sigma_{hkl} = a_{hkl} + b_{hkl} t$$

$$N_{in}(t) / N_{out}(t) \approx$$

$$e^{-(a_0+b_0 t)}\left[e^{-(a_{hkl}+b_{hkl}t)} + \left(1 - e^{-(a_{hkl}+b_{hkl}t)}\right)\int_{2d_{hkl}}^{\infty} R(\lambda', t)\, d\lambda'\right]$$

Where:

$$\int_{2d_{hkl}}^{\infty} R(\lambda', t)\, d\lambda' =$$

$$\frac{1}{2}\left[erfc\left(-\frac{t - t_{hkl}}{\sqrt{2}\sigma}\right) - exp\left(-\frac{(t - t_{hkl})^2}{\tau} + \frac{\sigma^2}{\tau^2}\right) erfc\left(-\frac{t - t_{hkl}}{\sqrt{2}\sigma} + \frac{\sigma}{\tau}\right)\right]$$

On the right it is possible to see the fit of the previous edge, with the presented model.
The uncertainty on the edge position (≈80μs) is high because of the noise.
The accumulation time was ~30min.

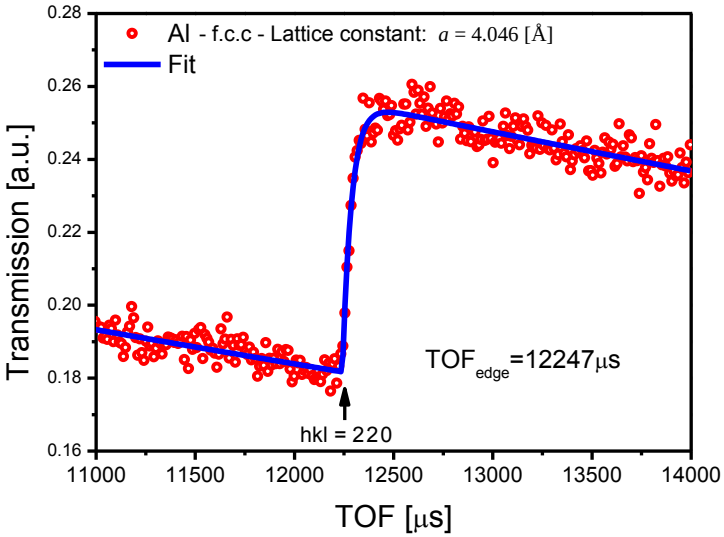

A ***neutron radiography*** is a 2-dimensional (2D-space resolved) measure of the neutrons number transmitted through a sample.

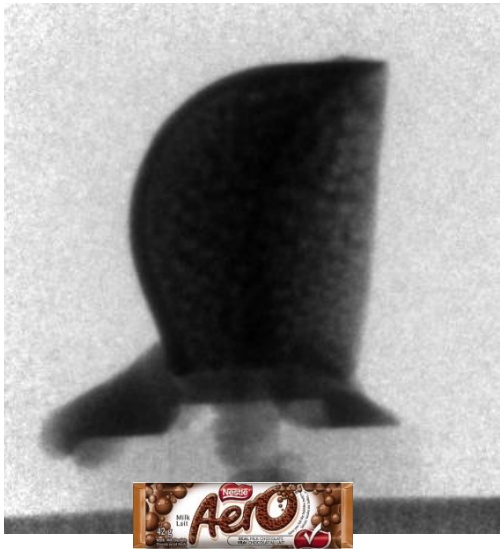

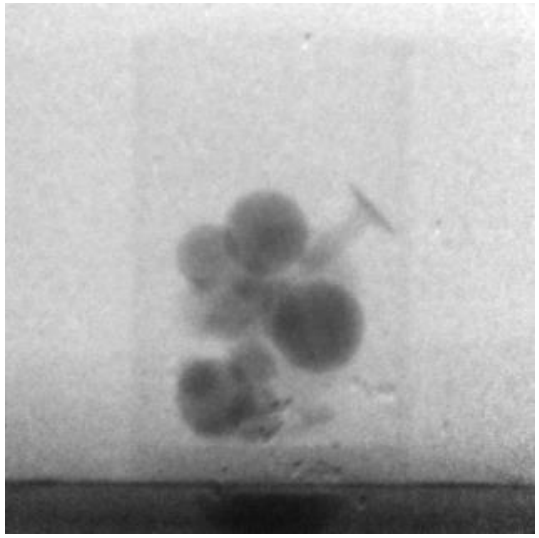

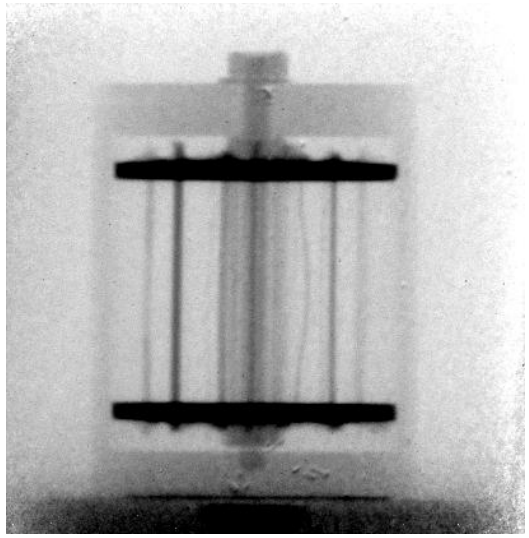

The intensity (**measured gray level**) at each image pixel in the time interval between t and $t+\Delta t$ after the pulse generation, gives a ***spatially resolved*** measure of the number of neutrons, with wavelengths between λ and $\lambda+\Delta\lambda$, transmitted through the sample.

A time resolved tomography is a 3-dimensional ***reconstruction*** of the intensity (**gray level**) at each image ***voxel*** in the time interval between t and $t+\Delta t$. In other words, a tomography could give a ***3-dimensional*** measure of the number of neutrons, with wavelengths between λ and $\lambda+\Delta\lambda$, transmitted through the sample.

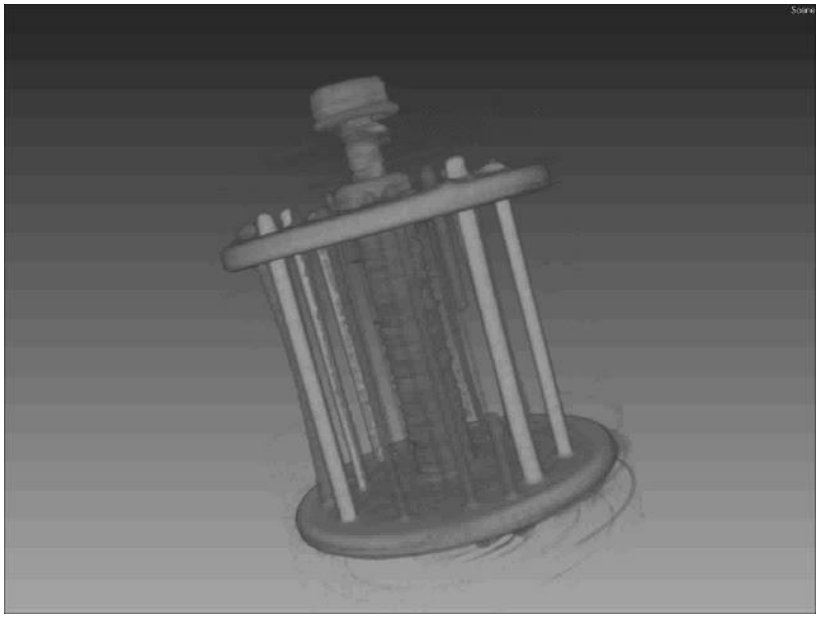

We could obtain a 2-D (or, in principle, even 3-D) map of the edge positions.

This, in turn, allows to obtain a map of the strains inside the sample.

Bended ***Cu*** samples

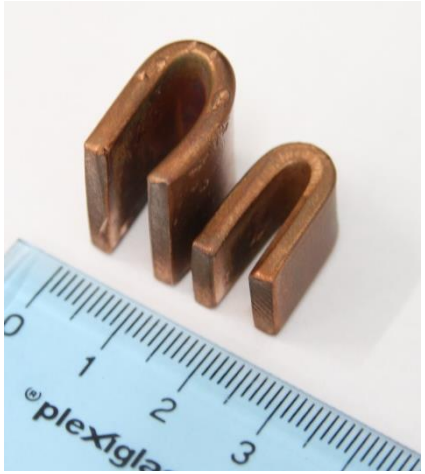

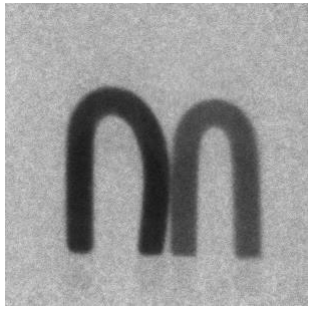

TOF = 8500***μs***
λ= 2.1691**Å**
ΔT=100***μs***
Exposure Time=250***s***

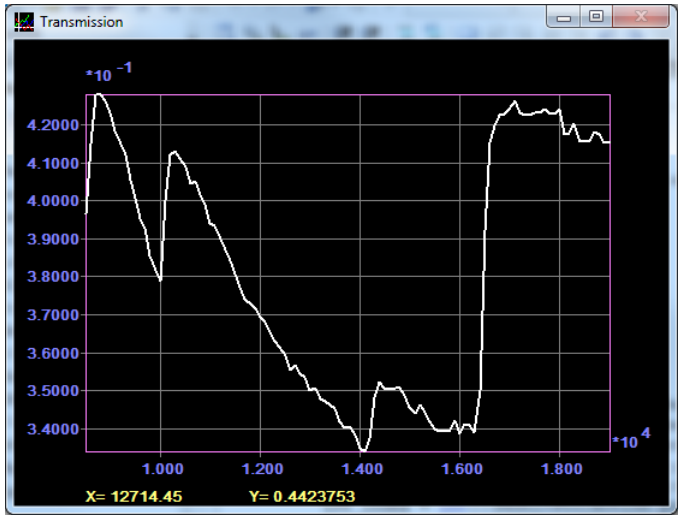

TOFs (8500-19000)***μs*** in 100***μs*** steps, corresponding to a wavelength range (2.17-4.85)**Å**

We have selected the edge at TOF~ 10000***μs*** (where the ROTAX beam intensity is near to its maximum) and we have fitted the data in order to verify point by point the edge position.

To obtain reasonable ***Signal/Noise*** ratios we need a consistent binning of the image (***30x30 pixels***).

λ=2.5774 **Å**

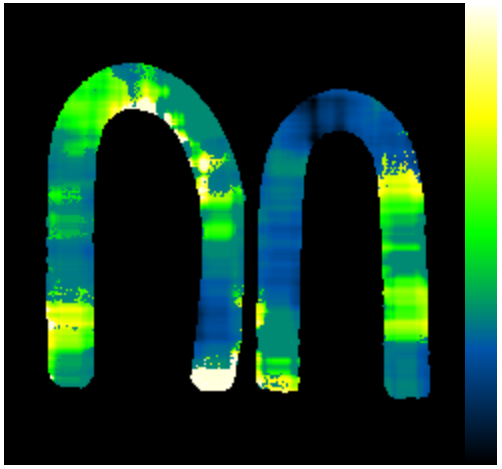

λ=2.5391 **Å**

How Neutron Imaging is done?

Most used scintillators are made by a mix of finely grounded powders of ***^{6}LiF*** and ***ZnS:Ag*** *or* ***ZnS:Cu*** mixed with an organic binder and deposited on a thin ***Al*** foil.

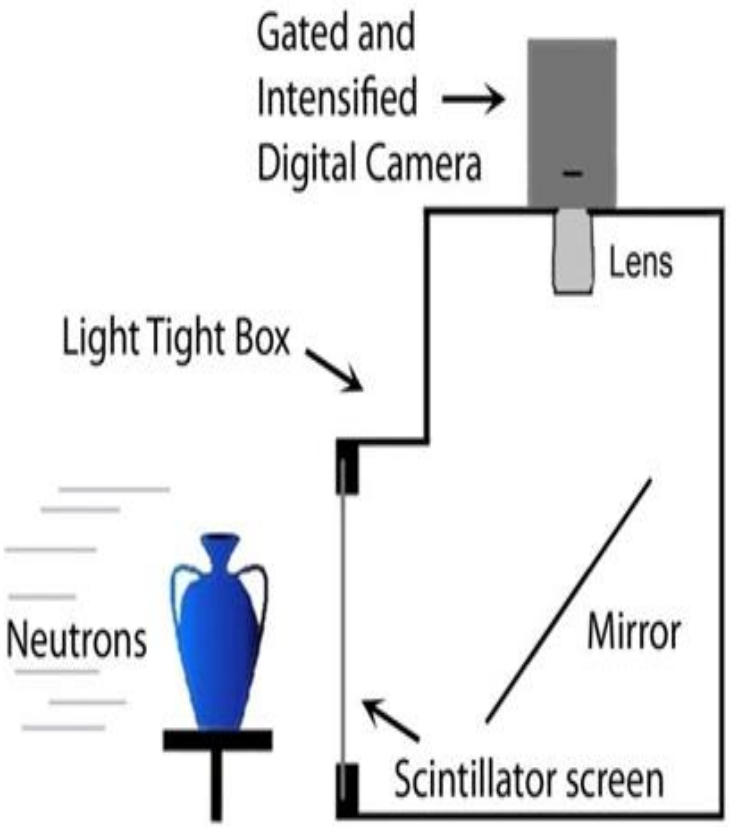

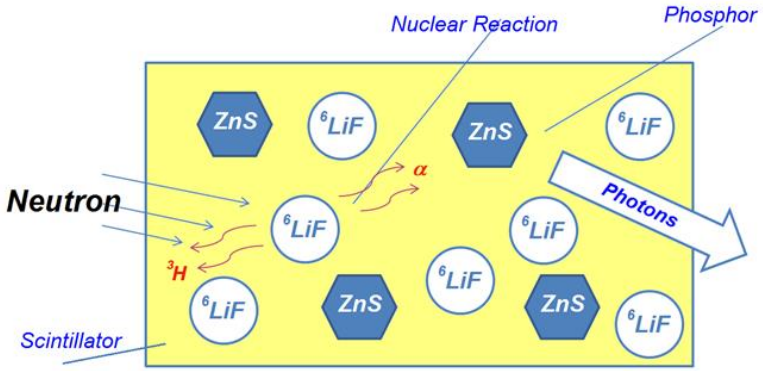

$$n + {}^6Li \rightarrow {}^4He(+2.05MeV) + {}^3H(+2.73MeV)$$

σ = 520 b

When the particles interact with the ***ZnS*** phosphor produce about ***160.000 photons per neutron*** C.W.E. van Eijk Nucl. Instr. And Meth. A **477** 383 (2002)

CCD image sensors

CCDs are ***very linear devices***: the number of collected electrons in a pixel is proportional to the number of incident photons.

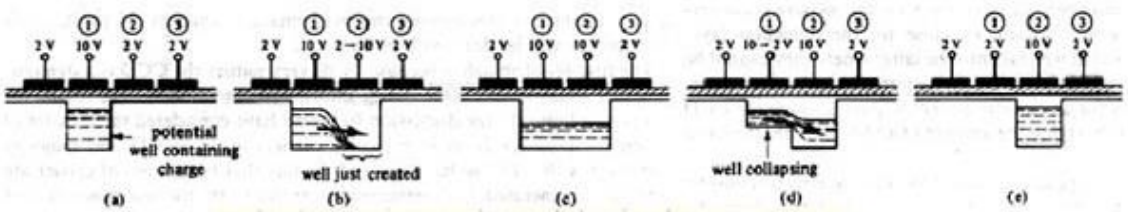

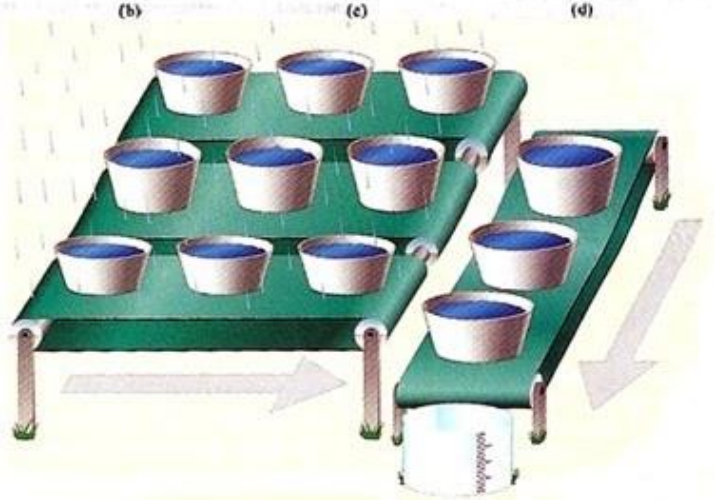

http://www.science.ca/images/scientists/s-boyle-infographic.jpg

The intrinsic ***noise*** of a ***CCD*** is low and can be reduced by ***cooling*** the sensor.

The main noise source, the ***readout noise,*** can reduced by slowing the readout process.

Fast CCD cameras exist that are capable of frame rates on the order of 1,000,000 frames per second (fps).

But the neutron flux (and, consequently, the light produced by the scintillator) is too low for using such camera for the time resolving imaging.

The requested time resolution can be obtained by interposing between the lens and the ***CCD*** sensor a ***<u>Gatable</u> Image Intensifier.***

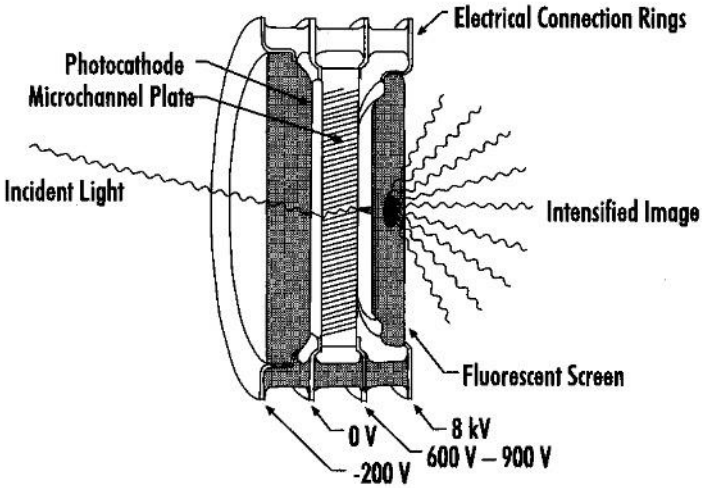

The micro channel plate is a thin disk (<1 mm thick) of honeycombed glass, and each of the honeycomb channels (~6-10µm) has a resistive coating.

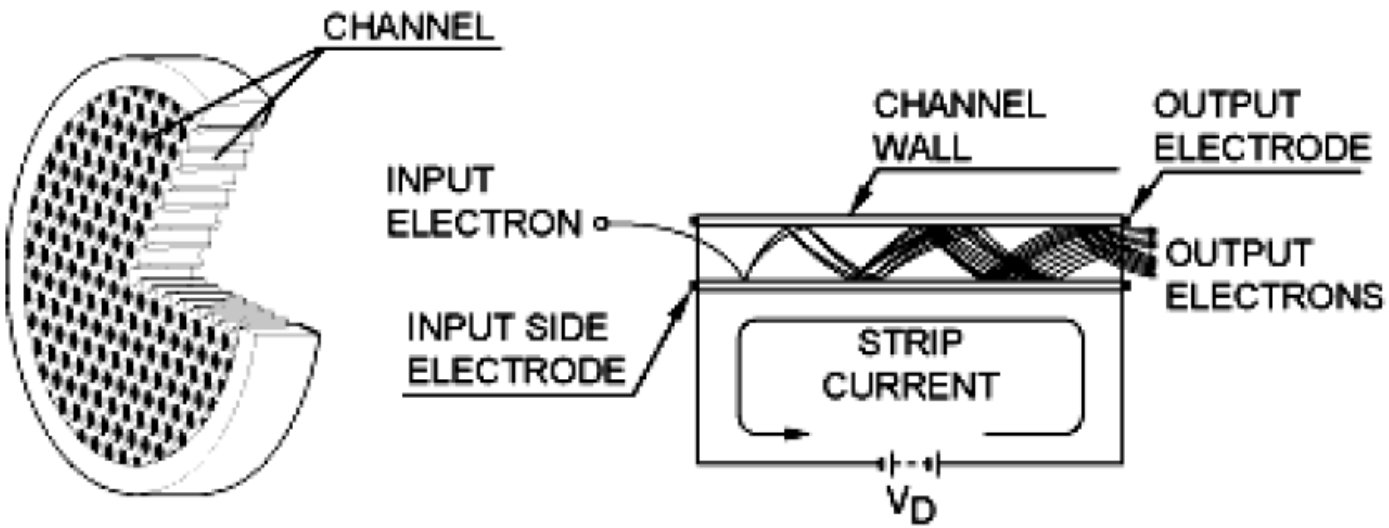

Across the micro channel plate a high potential is applied. The photoelectron will cascade down the channel producing secondary electrons; the resultant amplification can be up to 10^4.

The main amplification of an image intensifier is due to the electron cascade in the channel plate. Varying the voltage across the channel plate will control the gain.

Changing the voltage across the microchannel plate it is possible to completely stop the light (on/off ratio of the intensifier is $1:10^8$) reaching the CCD sensor.

We may control the exposure time by applying (high) voltage pulses across the microchannel plate.

Gate times <5ns can be reached so the requested time resolution (~10µs) can be easily obtained.

While short exposure times can be easily obtained with the gated intensifier, a problem arises because of the scintillators.

The commonly used ones (made of ^{6}*Li/ZnS and doped with Ag or Cu*) have very long decaying times.

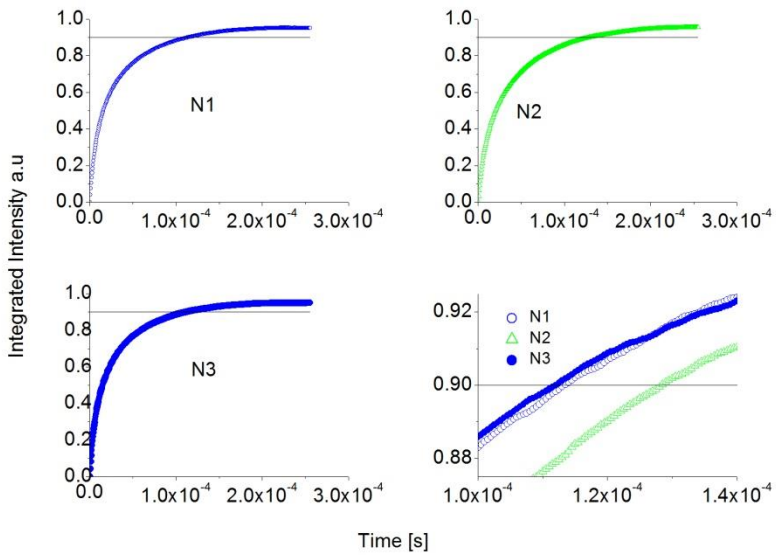

5% o the signal is still present after ~80µs and longer decaying times are found in scintillators doped with *Cu.*

We can still detect the presence of the Bragg edges but with a poor accuracy.

Energy selective imaging, with CCD and ^{6}*LiF/ZnS* scintillators can be used for contrast enhancement.

We have to acquire images at energies before and after a Bragg edge.

Cu-Fe Cube

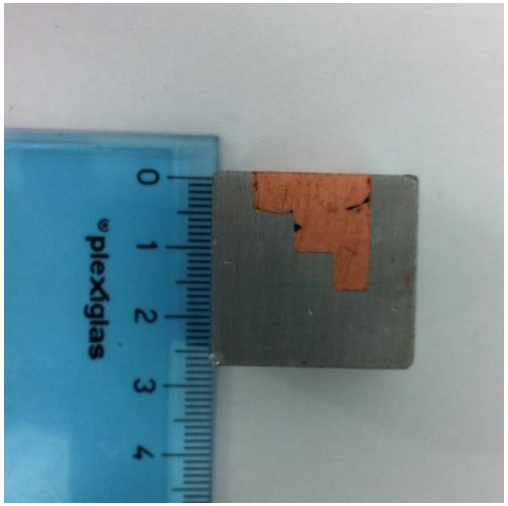

Contrast Inversion

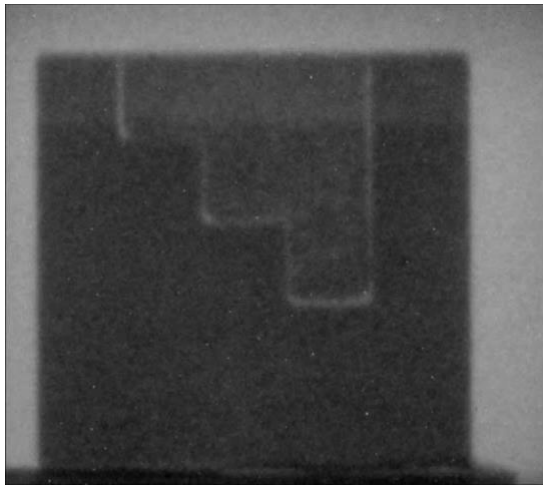

In the movie on the right three different *Cu* crystals are imaged at different wavelengths in the range 1.8-4.3Å.

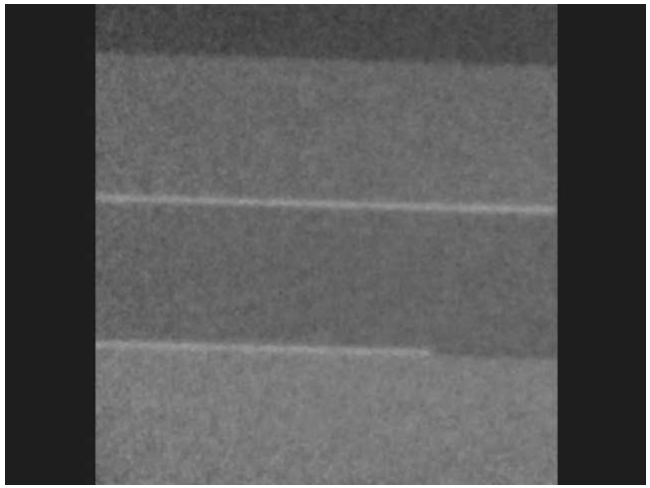

The images were acquired with a gated CCD coupled with a ^{6}*LiF/ZnS* scintillator.

It can be noted that the top crystal and the one in the middle are not homogeneous.

Each picture is a sum of many exposures, each ***25µs*** long, with a ***total exposure time of 0.48s*** (**480s of beam time** @40Hz). The sum is done on the chip to reduce the readout noise.

This procedure is called ***"Integrate on Chip"***.

A further disadvantage of this technique is that only one wavelength at time can be imaged.

A terrible waste of beam time !

At IMAT there will be, also, a different imaging detector developed by A. Tremsin and coworker [1].

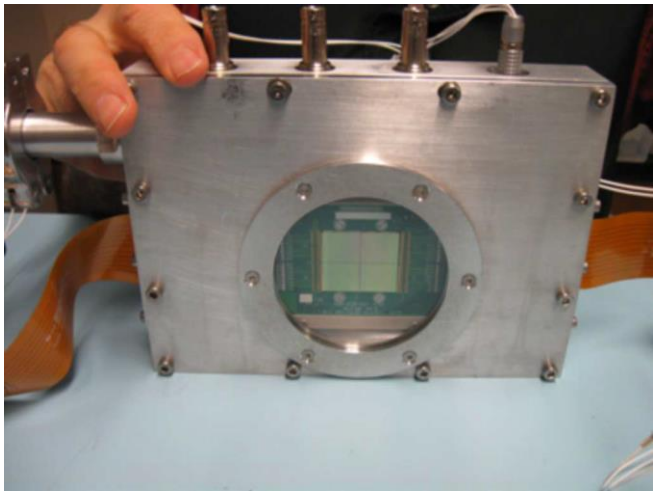

[1] IEEE Transactions on Nuclear Science, **60**, 578 (2013)

The sensor is based on ***neutron-to-charged particle*** conversion in ***^{10}B***-doped microchannel plates (***MCP***s)

The neutron detection exploits the ^{10}B(n, α) ^{7}Li reaction.

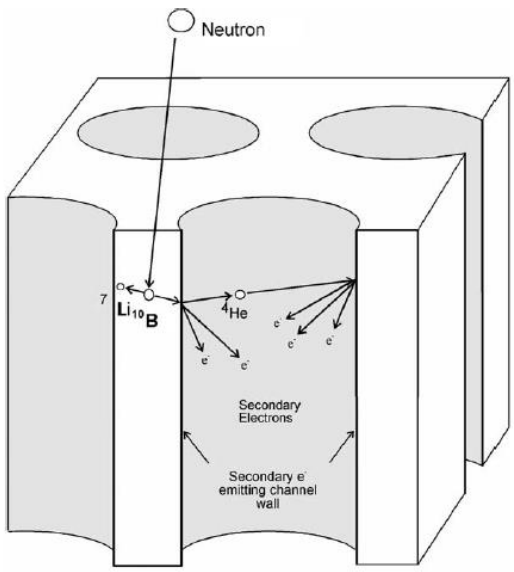

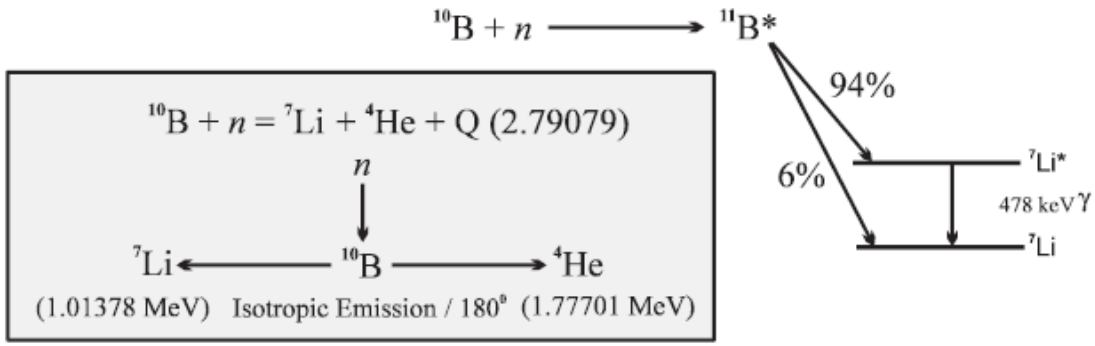

The micro channel plate is <1 mm thick, and each channel (~6-10μm) has a resistive coating.

A.S. Tremsin et al. *Nucl. Instr. and Meth.* A **539** 278–311 (2005)

The ***alpha*** and ***^{7}Li*** charged particle reaction products emerge from the channel wall surfaces into an open channel.

The heavy particles that cross the surface are accelerated by an external Electrical field.

A number of secondary electrons (~10^4) are generated to ***form a strong electron avalanche*** and, eventually, a measurable output pulse.

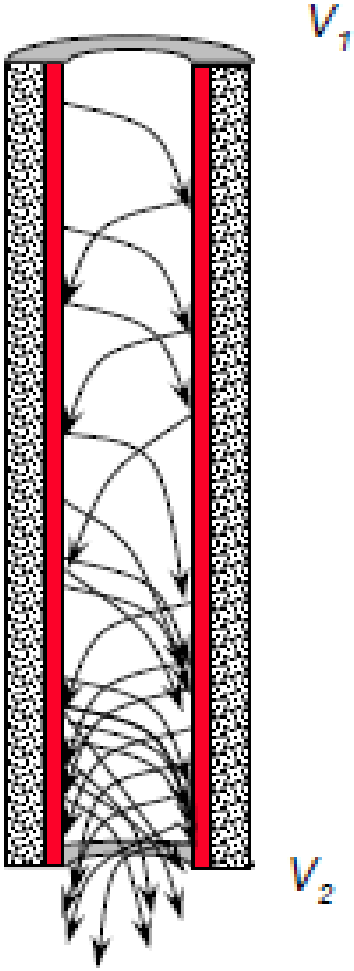

A.S. Tremsin et al. **IEEE NSS 2007, October 2007**

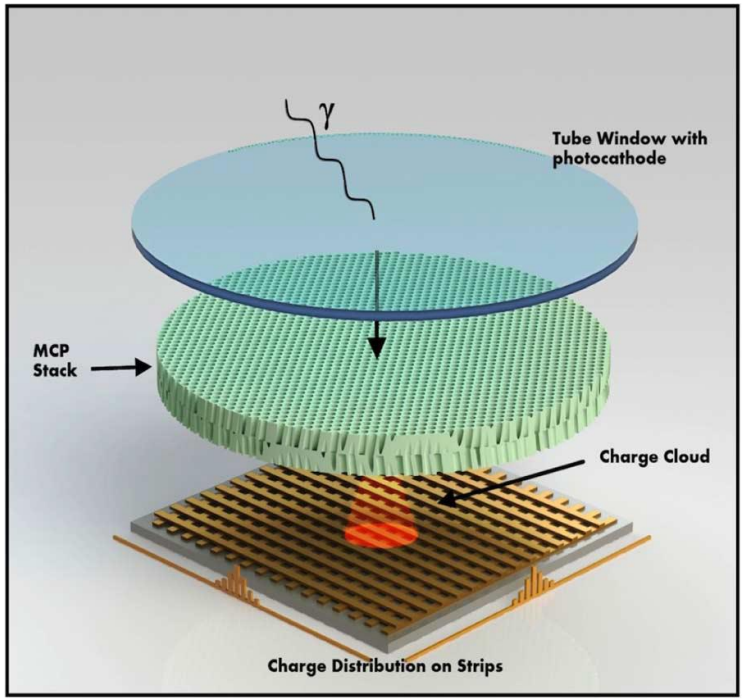

O. H. W. Siegmund et al.
IEEE Tr. On Nucl. Sci., **60**, 923 (2013)

The top MCP is 33 mm in diameter, 0.8 mm thick and has 8 µm pores on 10.5 µm centers (Nova Scientific, Inc.).

$^{10}B(n,\alpha)^{7}Li$ reaction,
$\sigma_{thermal}$=3837 barns

The bottom MCP is 50 mm in diameter, 0.6 mm thickness and has 10 µm pores hexagonally packed on 12 µm centers (Hamamatsu Photonics).

The neutron sensing *MCP*s are combined with a fast readout ***CMOS*** device, developed at CERN: ***Timepix***.

It has ***256x256*** pixels with an active area of ***14x14mm²*** and it is *3-side buttable*.

The pixel size is *55x55 μm²* and each pixel has an amplifier, a variable threshold and a 14 bit counter that can be programmed to ***count hits*** or to measure ***arrival time*** of the a particle.

The parallel readout allows readout speeds of up to 1200 frames per second with ~300μs dead time for each frame. After that the Timepix is ready to register new events by opening the electronic shutter which enables pixel counters.

The third generation of Timepix will have 2 counters per pixel allowing to work in simultaneous read/write mode (one counter is read out while the other counts).

Pixel architecture

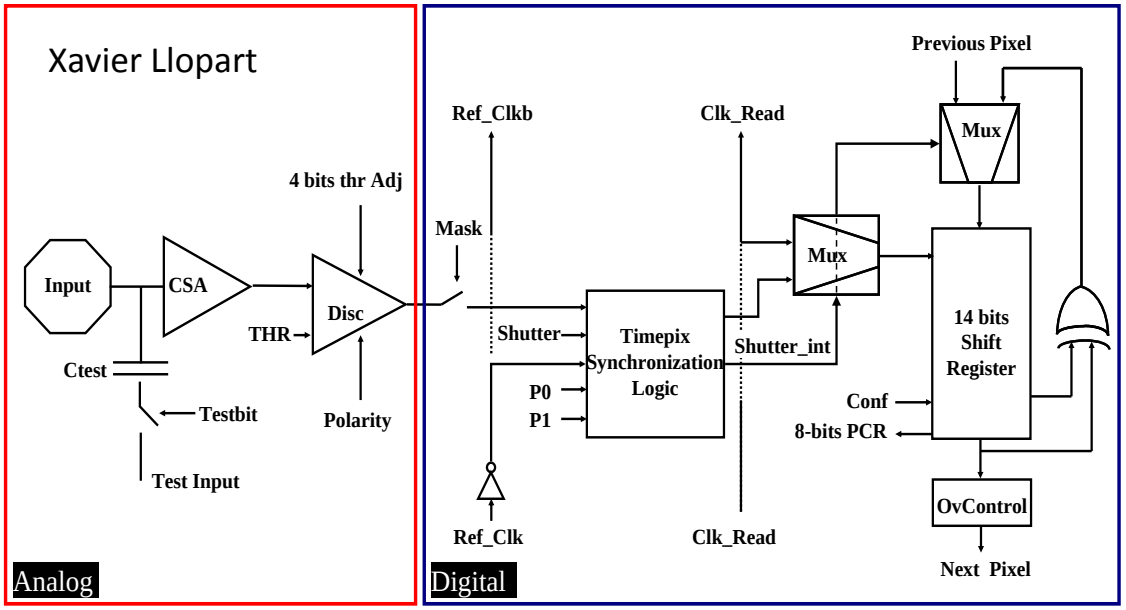

- A single threshold with one 4-bit threshold adjustment DAC.
- Each pixel can be configured independently in three different operation modes:
  - Arrival time mode
  - Energy mode (TOT)
  - Event counting

TIMEPIX architecture

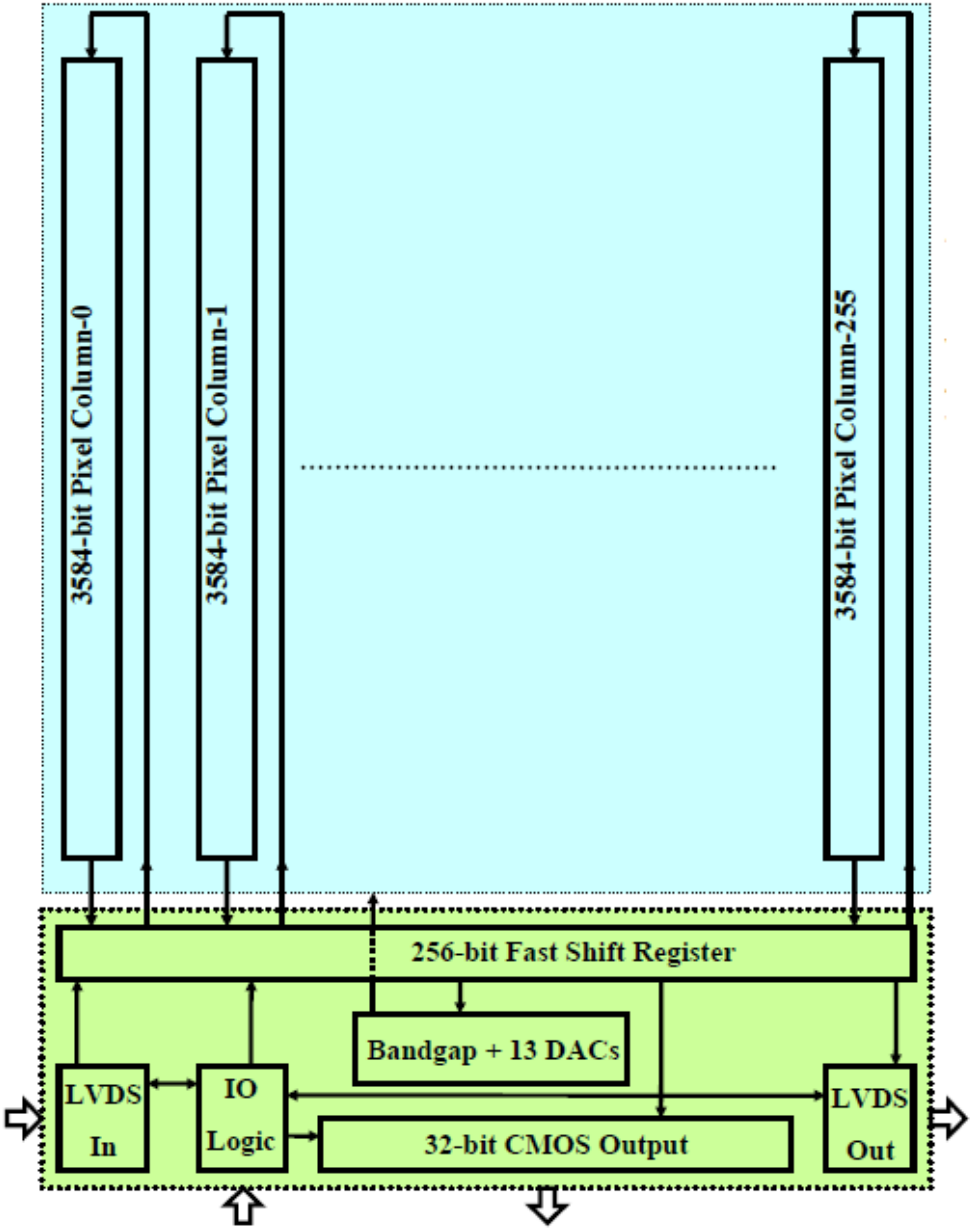

Xavier Llopart

3th generation MEDIPIX/TIMEPIX

R. Ballabriga et al.
Nucl. Instr. and Meth. A 633 (2011) S15–S18

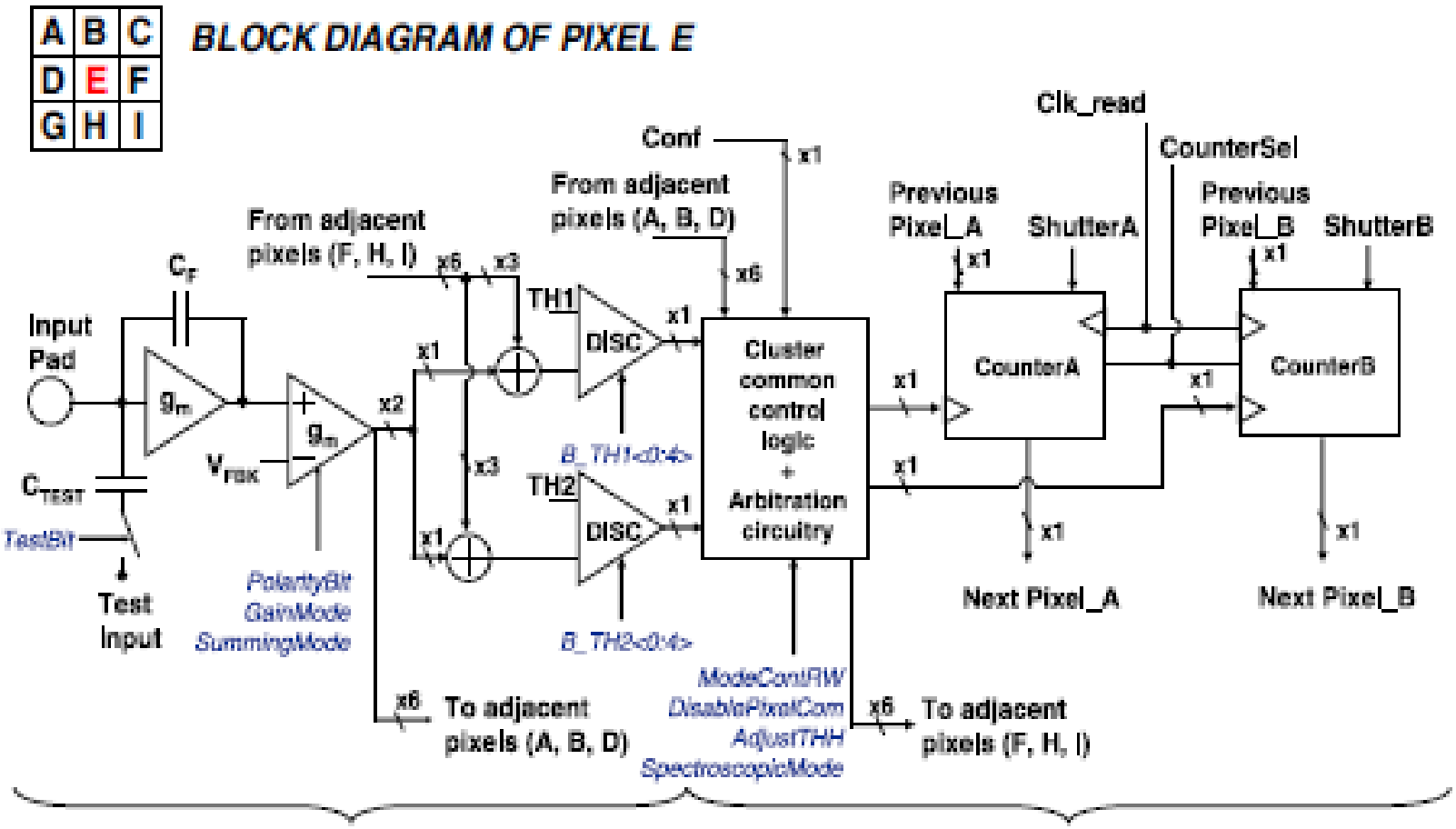

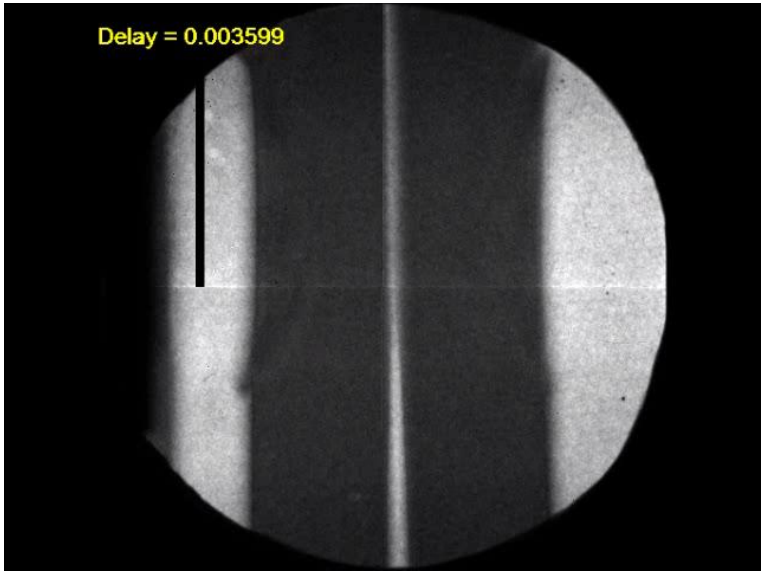

Data collected at ENGIN-X by Anton Tremsin

Time width of each image = 10.24µs
Number of triggers acquired = 82798
Equivalent acquisition time = 69min
Source-Sample distance = 50m

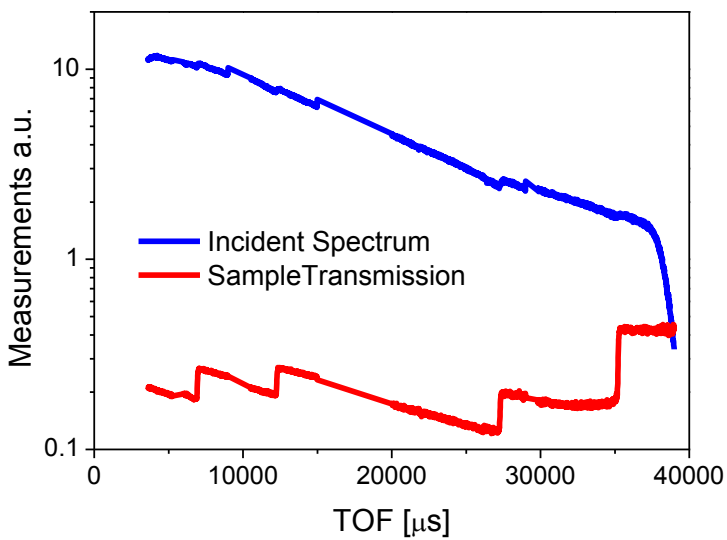

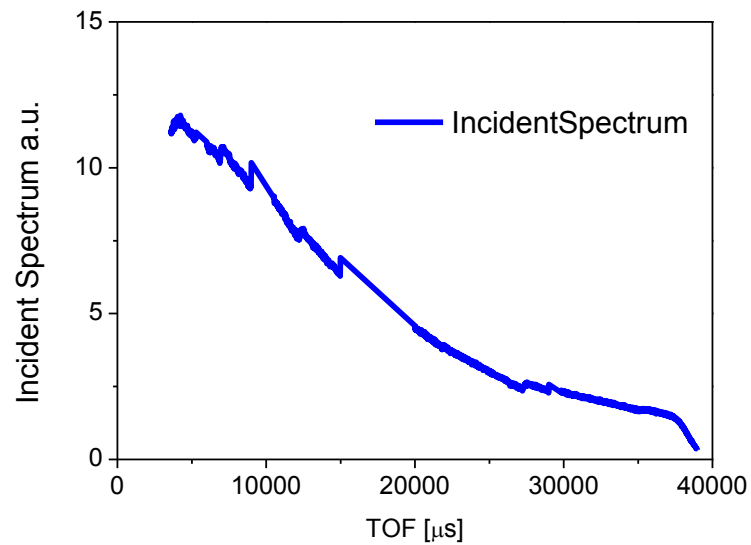

The detector is capable of a spatial resolution **~10µm** at event rates up to ~3MHz, using an event *centroiding* algorithm, and of ~ 55µm at event rates greater than 200MHz [1].

[1] A. S. Tremsin IEEE Trans. on Nucl. Sci., **60**, 578 (2013)

PImMS (Pixel Imaging Mass Spectrometry) is a new, promising sensor developed in Oxford, originally for applications in imaging mass spectrometry. C. Vallance et al. ***Phys.Chem.Chem.Phys.*** 16, 383 (2014)

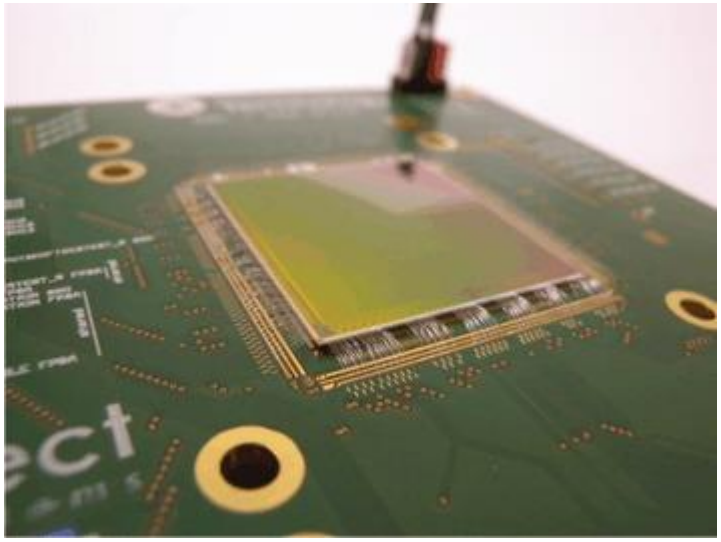

324×324 pixels each 70×70μm^2

Each pixel is configured to record particle arrival times. The sensor can store up to **four arrival times per pixel** to allow detection of multiple particles on each TOF cycle.

The sensor can detect high energy charged particles directly but, it is configured primarily as a visible light sensor, and is most commonly used in combination with a MCP/phosphor position-sensitive detector.

The “Messina Team”

Left to right:

- **Roberto Caruso**
- **Giuseppe Spinella**
- **Vincenzo Finocchiaro**
- **Gabriele Salvato**
- **Francesco Aliotta**
- **Rosa Ponterio**
- **Cirino Vasi**
- **Domenico Arigò**
- **Dario Tresoldi**
- **Giuseppe Lupò**

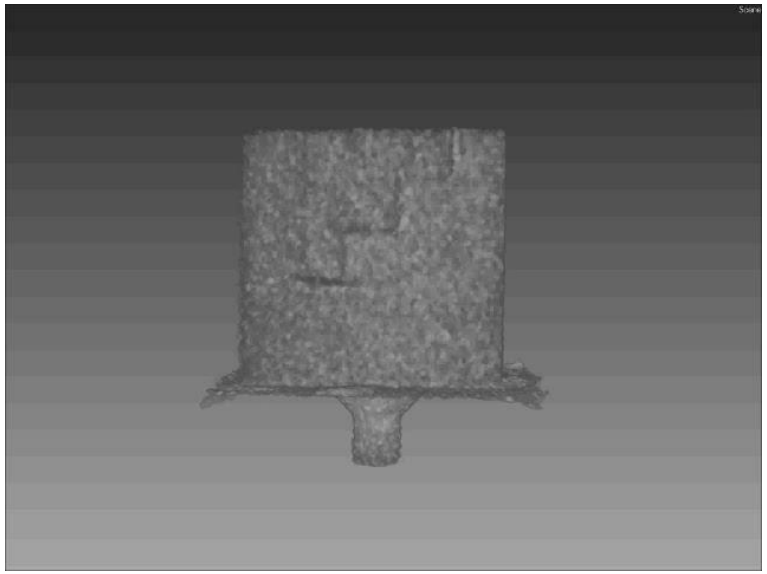

TANK YOU

Spares

The Box of the camera box

What will we found inside ?

Surprise ! The camera is Intact !

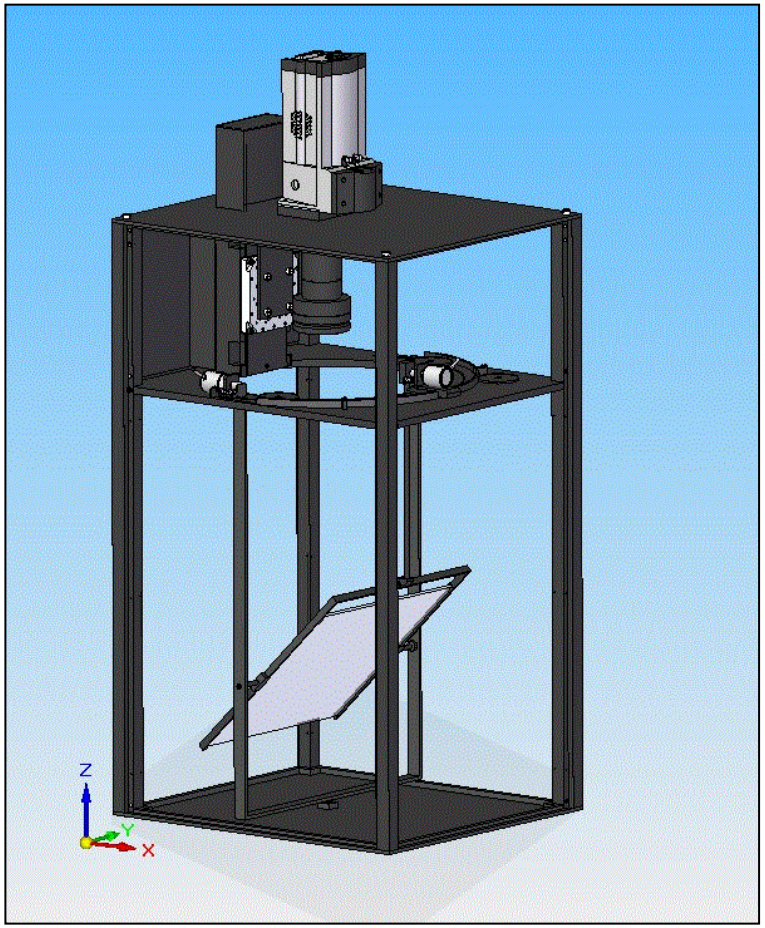

Lens	Field of View mm^2	Pixel resolution
50mm f/1.2	211.5x211.5	0.20 mm
85mm f/1.4	112.7x112.7	0.11 mm
105mm f/2.5	85.5x85.5	0.08 mm
135mm f/2.0	59.5x59.5	0.06 mm

To Change the lens

Fast mount and release
(ball-spring mechanism)

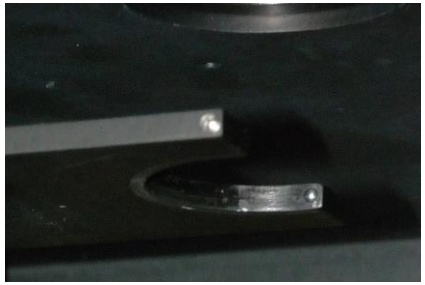

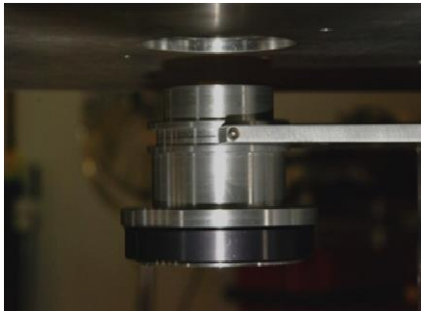

Lens in ***mounting*** position

Lens in ***focused*** position

Auto Focusing

V.Finocchiaro et al. Rev. Sci. Instrum. **84**, 093701 (2013)

Laser pointer (Global Laser Ltd. mod. Cameo)
+ Diffracting lens

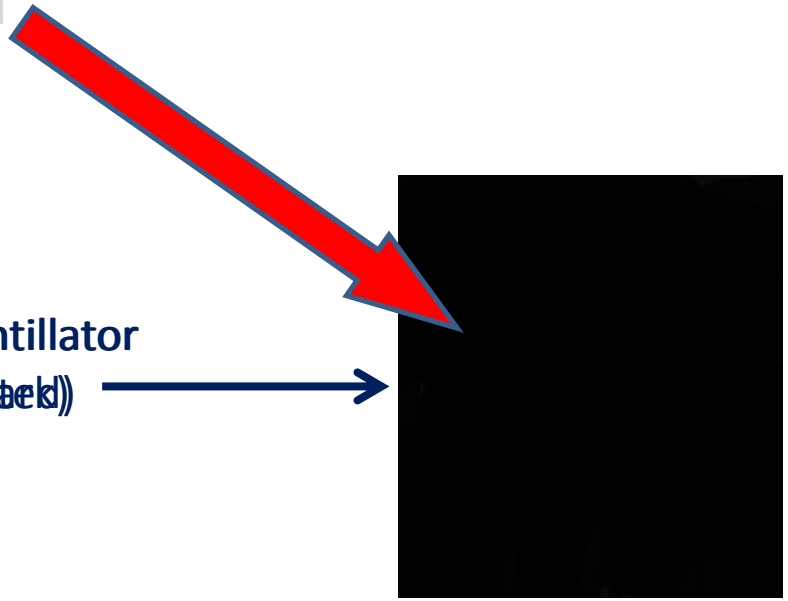

^{6}LiF/ZnS scintillator
(illuminated)